Evolution in Electrical and Electronic Engineering Vol. 3 No. 2 (2022) 508-516

EEEE

Homepage: http://publisher.uthm.edu.my/periodicals/index.php/eeee
e-ISSN : 2756-8458

Computational Study of Excitation Coil for Magnetic Particle Imaging Application Using JMAG Software

Muhammad Fakhrul Syazwan Mohd Fauzi[1], Nurmiza Othman[1]*

[1]Faculty of Electrical and Electronic Engineering,
Universiti Tun Hussein Onn Malaysia, Batu Pahat, 86400, MALAYSIA

*Corresponding Author Designation

DOI: https://doi.org/10.30880/eeee.2022.03.02.060
Received 27 June 2022; Accepted 21 September 2022; Available online 30 October 2022

Abstract: Magnetic particle imaging (MPI) is a novel tomographic approach for three-dimensional (3D) imaging that employs magnetic nanoparticles (MNP) as a tracer. MPI is made up of three major components: MNP, magnetic coils, and an image reconstruction approach. The scanning process is made more difficult and constrained by the complicated topology of the skin surface, the physical qualities, configuration, and the dimension of the coil, and the high input current for excitation. By increasing the magnetic field induction, image quality may be increased. This project focused on the computational study of excitation coil for MPI application by using JMAG software. Through this study, the parameter and specifications of the excitation coil were developed and simulated using JMAG software. Two types of design are being simulated in this project, Design A and Design B. These two designs have a similar shape but Design B is divided into small sub-coils. Both designs are simulated with the ferrite and without ferrite at the core of the excitation coil to see the difference in the magnetic field produced by the excitation coil. From the simulation, the maximum value of contour produced by the excitation coil was investigated to study the distribution of magnetic field induction around the coil. As a result, the difference value with ferrite and without ferrite produced by design A is 106.73µT and the difference value with ferrite and without ferrite produced by design B is 105.21 µT. For this project used two types of material for the excitation coil core which is used ferrite and without ferrite can be summarized and can be developed the excitation coil core using ferrite. This project has proven that ferrite used as excitation coil core produced a stronger maximum value of magnetic flux density than excitation coil core that did not use ferrite for both designs A and B. Finally, a portable single-sided MPI scanner with a simple coil arrangement, compact size, and low current can be constructed for MPI applications to generate a high magnetic field induction in the future.

Keywords: Magnetic Field, Excitation Coil, JMAG Software, Ferrite

**Corresponding author: nurmiza@uthm.edu.my*

1. Introduction

Magnetic particle imaging (MPI) was introduced in the early 2000s [1]. MPI uses the nonlinear magnetic response of magnetic nanoparticles in alternating fields to measure their distribution in tissue. MNP tracers' magnetic field properties affect MPI's signal intensity, spatial resolution, and temporal resolution. MPI uses a magnetic gradient field, called a selection field, to saturate superparamagnetic iron oxide (SPIO) magnetization beyond a central field-free zone. A fast-varying excitation/drive field swiftly moves the FFL to form a picture. Large fields of vision need slower shift fields and mechanical translation. As the FFL moves to form a signal, SPION magnetization fluctuates nonlinearly. Time-varying magnetization induces a voltage in the receiver coil, which is allocated to the FFL location to generate a magnetic particle picture. Induced voltages are proportional to the number of SPIONs at the FFL, enabling SPION quantification. MPI's low-frequency magnetic fields are neither created nor reduced by biological tissue, enabling optimum contrast regardless of source depth [2].

Previous studies discovered that the MPI's magnetic nanoparticle composition, magnetic coil system (excitation coil and detecting coil), and image reconstruction method were all important [3]. Gleich and Weizenecker designed a high-resolution MPI system prototype in 2005 [4]. Settel et al. introduced a single-sided MPI system in 2008 that scans a subject from one side [5]. Meribout and Kalra proposed a safe, portable MPI system in 2020. The apparatus uses a Halbach array of neodymium-iron-boron (NdFeB) magnets to create a strong homogeneous magnetic flux. This elevates magnetic flux density in the FOV over MNP's saturation threshold [6].

MPI begins by injecting MNPs into a subject. The Langevin theory can forecast the MNPs' (SPION) magnetization. After being ignited by the excitation coil, MNPs concentrate in the detection coil's target region. The picture reconstruction step uses receive coil data to locate and quantify MNPs [3]. Shahkhirin et al. [7] suggested a Maxwell coil pair and vertically stacked sub-coil that can create a strong and uniform magnetic field of 17.5759 T. In this project, JMAG software will be used to create and simulate different excitation coil types. The simulation results based on the excitation coil's magnetic field induction will be analysed to determine if AC signal excitation improves the model's quantitative and qualitative values.

The MPI system application's reconstruction image quality may be affected by the complex surfaces of the human body’s skin. The magnetic field intensity at the MNPs placed under the body surface is weak and inhomogeneous due to the design, size, and material chosen for the available excitation coil. Furthermore, the magnetic coils employed are often huge and have a cave-form design, which makes them unsuitable for use as portable scanning instruments. Previous research [7] proposed a novel technique to improve magnetic field induction and homogeneity using DC signals. This project will further investigate the model by employing an AC signal to obtain the magnetic field induction signal. As a result, the focus of this project will be on developing an excitation coil that will provide better magnetic induction strength to the MNPs accumulated under the body surface.

2. Materials and Methods

For modeling a three-dimensional (3D) electromagnetic model, JMAG software has a lot of functions. The magnetic field induction was determined using an excitation coil that was designed and simulated in this study. The excitation coil design and simulation flowchart are shown in Figure 1. First, JMAG software was used to put up the coil's shape, material, size, and arrangement.

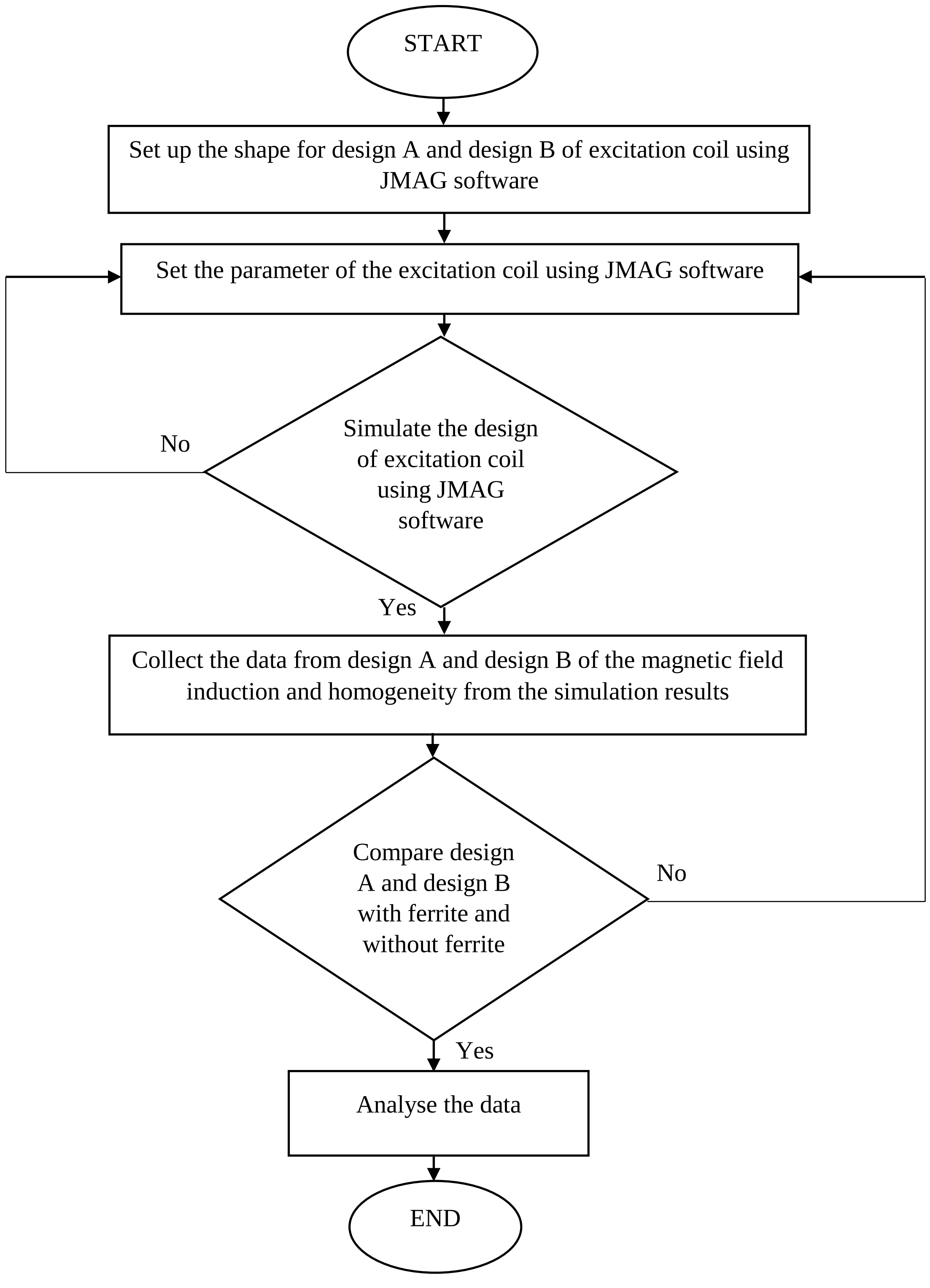

Figure 1: The excitation coil design and simulation flowchart

The cylindrical shape was chosen as the coil shape because prior research has shown that this shape can create a strong magnetic field induction [7]. Copper was used for the coil because of its high corrosion resistance and excellent electrical and thermal conductivity. Small electrical resistance results in good electrical conductivity. The less electrical resistance there is, the simpler it is for electricity to pass through the wire. Copper is a strong heat conductor because it is resistant to corrosion and has a high melting point. As a result, the coil can endure extreme temperatures.

Second, set a parameter for design A and design B of the excitation coil and a steady current source was used to establish a magnetic field in the coil. To avoid the heating effect, which might injure patients, the current amplitude must be kept low. Third, after passing the verification step, the coil design was simulated using JMAG software and the coil design created the magnetic field induction and homogeneity. Forth, the data being collected from design A and design B throughout the maximum value produced by contour plot when used ferrite and without ferrite at the excitation coil. Fifth, the data being compared from the magnetic field induction and homogeneity produced by design A and design B. The comparison is done with ferrite and without ferrite. Finally, the simulation results were then examined and analysed in terms of magnetic field induction and homogeneity. Table 1 and Figure 2 show the specification and parameters for Design A and Table 2 and Figure 3 for Design B.

Table 1: Specification and parameters for Design A

Specification	Parameter
Current, *I* (A)	0.8
Length of coil, *L* (mm)	70
Inner radius of coil, *a* (mm)	10
Outer radius of coil, *b* (mm)	50
Wire diameter, (mm)	1
Material	Copper
Shape	Cylinder

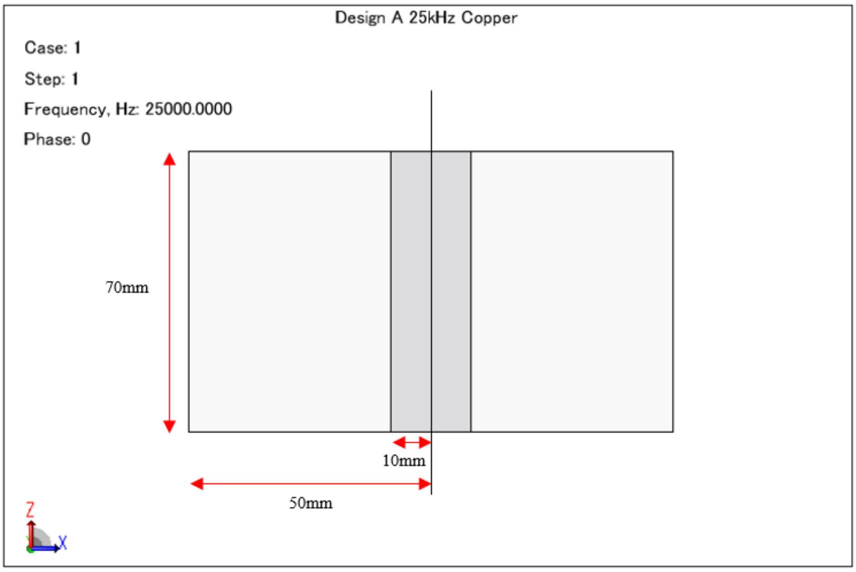

Figure 2: Design A

Table 2: Specification and parameters for Design B

Specification	Parameter
Current, I (A)	0.8
Length of oil, L_2 (mm)	14
Total Length of Coil, L (mm)	70
Inner radius of coil, a_E (mm)	10
Outer radius of coil, b_E (mm)	50
Wire diameter, (mm)	1
Material	Copper
Shape	Cylinder

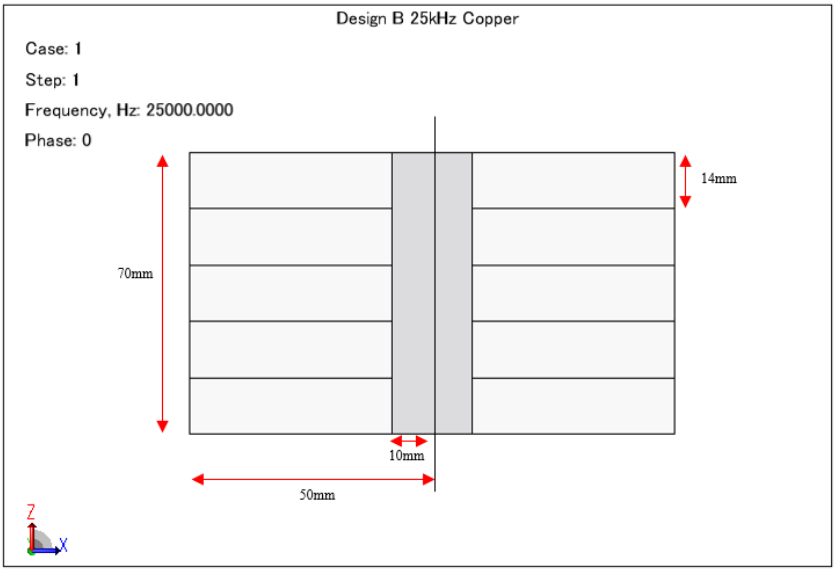

Figure 3: Design B

3. Results and Discussion

For results and discussion, the maximum value of magnetic flux density of the contour plot is recorded. The value is based on the 'phase' that is stated in JMAG software. The 'phase' represents for complete wave cycle for the waveform. The results are based on the core conditions in the excitation coil, without ferrite and with ferrite.

3.1 Design A without Ferrite

From Figure 4, the maximum and minimum value of the vector plot is zero because of the starting phase of one cycle of the waveform. The line of the vector plot moves from the bottom and to the top of the coil. The maximum value of magnetic flux density of the contour plot is shown which the maximum value is 7.9991 µT and the minimum value is 3.1234E – 10 T.

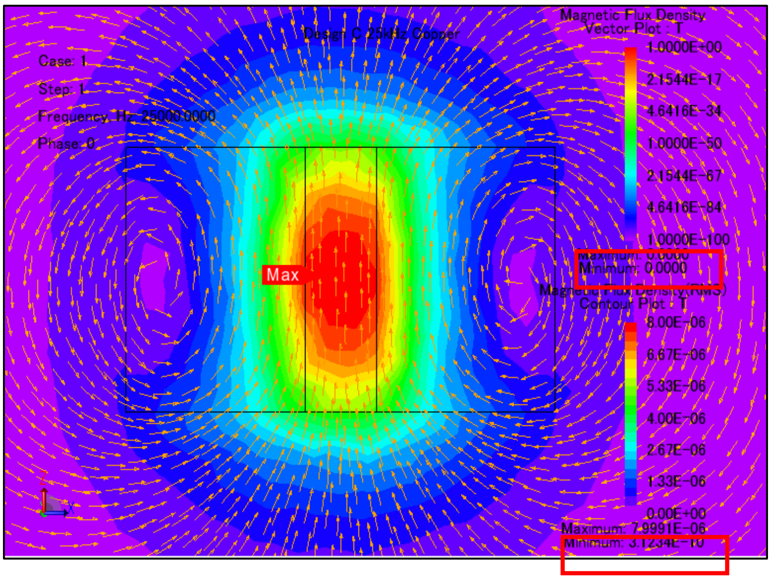

Figure 4: Magnetic field induction and homogeneity produced from design A without ferrite

3.2 Design A with Ferrite

Figure 5 shows the value of magnetic flux density produced when ferrite is used as a core. The vector line enters the coil from bottom to top. The maximum value of magnetic flux density of the vector plot is shown this time. The maximum value is 2.0097E – 14 T and the minimum value is zero. While the value of magnetic flux density of the contour plot is shown with a maximum value is 114.73 µT and a minimum value is 5.2825E – 10 T.

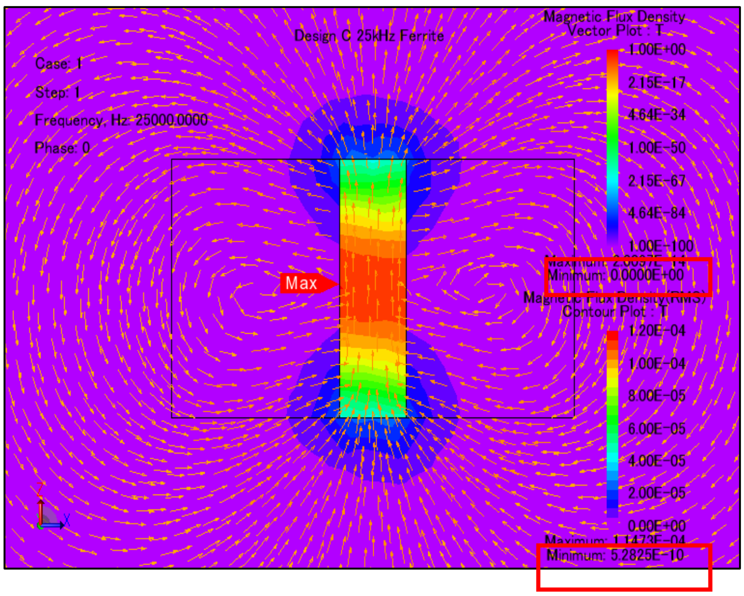

Figure 5: Magnetic field induction and homogeneity produced from Design A with Ferrite

3.3 Design B without Ferrite

Figure 6 shows the magnetic field induction and homogeneity produced by the excitation coil in design B without ferrite. Design B is similar to design A but the excitation coil of design B is divided into smaller sub-coils. The maximum and minimum value of magnetic flux density of the vector plot shown is zero with the line vector moving from the bottom and going to the top. The maximum and minimum value of magnetic flux density of the contour plot is shown which the maximum value being 8.0417 µT and the minimum value being 2.1090E – 10 T.

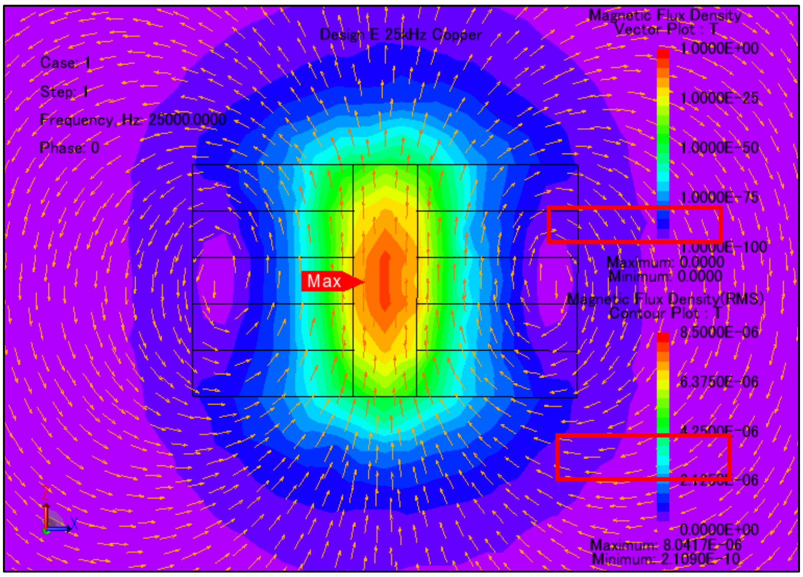

Figure 6: Magnetic field induction and homogeneity produced from Design B without Ferrite

3.4 Design B with Ferrite

Figure 7 shows the value of magnetic flux density produced when ferrite is used as a core. The vector line enters the excitation coil from the bottom to the top. The value of magnetic flux density of vector plot is shown with the maximum value is 3.5527E – 15 T and the minimum value is zero. The value for magnetic flux density for the contour plot is also shown which a maximum value is 113.25 μT and a minimum value is 2.3834E – 10 T.

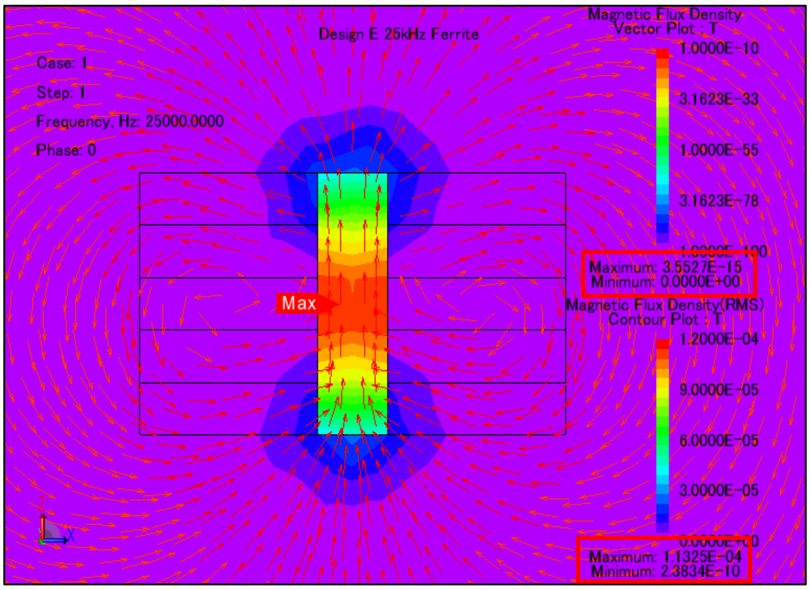

Figure 7: Magnetic field induction and homogeneity produced from Design B with Ferrite

3.5 Magnetic field generated from Design A

Table 3 shows a comparison of the maximum value of magnetic flux density in different materials used for the core of the excitation coil which is with ferrite and without ferrite in design A.

Table 3: Magnetic field induction generated using 25 kHz in Design A

Core	Maximum value of Magnetic Flux Density (µT)
Without Ferrite	7.9991
With Ferrite	114.73

3.6 Magnetic field generated from Design B

Design B is similar to design A but design B has been divided into smaller sub-coils. Table 4 shows a comparison of the maximum value of magnetic flux in different materials used for the core of the excitation coil which is without ferrite and with ferrite in design B.

Table 4: Magnetic field induction generated using 25 kHz in Design B

Core	Maximum value of Magnetic Field Density (µT)
Without Ferrite	8.0417
With Ferrite	113.25

3.7 Discussion

From Table 3 and Table 4, the maximum value of magnetic flux density for the contour map for both designs A and B have a huge gap between the two core materials. In design A, without ferrite, the maximum value of magnetic flux density of the contour plot produced 7.9991 µT while with ferrite the maximum value is 114.73 µT. The difference value of magnetic flux density for the contour plot between each core is 106.73 µT. Same with design B, the maximum value of magnetic flux density for contour plot for both cores, with ferrite and without ferrite has a huge gap. Without ferrite, the maximum value of magnetic flux density for the contour plot produced 8.4017 µT while with ferrite, the maximum value of magnetic flux density is 113.25 µT. The difference value of magnetic flux density for the contour plot between each core is 105.21 µT. Ferrite has higher relative magnetic permeability than copper. Ferrite relative permeability is 16 – 640 and copper relative permeability is 0.999994 [8]. The gap that happens when ferrite is used as a core can affect the magnetic field by maximizing the amount of magnetic flux density brought about by the passage of magnetising current into the core of the magnet. This effect can be seen from the magnetic flux density when the ferrite core was used as a core in both designs.

4. Conclusion

Based on the discussion, it can be simplified that the ferrite that is used as a core of the excitation coil produced strong magnetic field induction and homogeneity based on the value of magnetic flux density. Both designs A and design B shows that the value of magnetic flux density produced from the excitation coil when used ferrite as a core produced a strong magnetic field than when the excitation coil did not ferrite as a core. For design A, when ferrite is used as a core the value is 114.73 µT while without ferrite the value is 7.9991 µT. For design B, the value of the magnetic field when ferrite is used as a core is 113.25 µT but when ferrite is not used as a core the value is 8.0417 µT. For further development, ferrite can be used as a core for excitation coil used in MPI system applications because using ferrite as a core improves performance by giving high permeability to the coil. It causes their magnetic field and inductance to increase.

Acknowledgement

The authors would also like to thank the Faculty of Electrical and Electronic Engineering, Universiti Tun Hussein Onn Malaysia for its support.

References

[1] L. C. Wu et al. “A Review of Magnetic Particle Imaging and Perspectives on Neuroimaging.” AJNR. American journal of neuroradiology vol. 40, no. 2 pp. 206-212, 2019. doi:10.3174/ajnr.A5896

[2] S. Sarangi and A. Brazdeikis, "Interacting magnetic nanoparticle clusters for enhancing magnetic particle imaging performance," 2013 International Workshop on Magnetic Particle Imaging (IWMPI), 2013, pp. 1-1, doi: 10.1109/IWMPI.2013.6528380.

[3] M. F. S. Birahim, N. Othman, N., M. R. M. Tomari, “Design and Simulation Study of Excitation Coil System with Different Array Configurations for Magnetic Particle Imaging Application,” International Journal of Integrated Engineering, vol. 12 no. 3, pp. 278-286, 2020.

[4] B. Gleich, B., J. Weizenecker, J. “Tomographic imaging using the nonlinear response of magnetic particles,” Nature, vol. 435, no. 7046, pp. 1214-1217, 2005. doi:10.1038/nature03808.

[5] T. Sattel, et. al. “Single-sided device for magnetic particle imaging,” Journal of Physics D: Applied Physics, vol. 42, no.2, 022001, 2008.

[6] M. Meribout, M. Kalra, “A portable system for two dimensional magnetic particle imaging,” Measurement, vol. 152, February 2020, 107281. doi: 10.1016/j.measurement.2019.107281.

[7] M. F. S. Birahim, “Alternative Design of Coil System Using Ansys Maxwell for Three-Dimensional Scanning of Human Body”, Universiti Tun Hussein Onn Malaysia (Master Thesis 2021).

[8] Engineering ToolBox, (2016). *Permeability*. [Online] Available at: https://www.engineeringtoolbox.com/permeability-d_1923.html [Accessed: 16-Sep-2022].